

# Catalysis Science & Technology

Accepted Manuscript



This is an *Accepted Manuscript*, which has been through the Royal Society of Chemistry peer review process and has been accepted for publication.

*Accepted Manuscripts* are published online shortly after acceptance, before technical editing, formatting and proof reading. Using this free service, authors can make their results available to the community, in citable form, before we publish the edited article. We will replace this *Accepted Manuscript* with the edited and formatted *Advance Article* as soon as it is available.

You can find more information about *Accepted Manuscripts* in the [Information for Authors](#).

Please note that technical editing may introduce minor changes to the text and/or graphics, which may alter content. The journal's standard [Terms & Conditions](#) and the [Ethical guidelines](#) still apply. In no event shall the Royal Society of Chemistry be held responsible for any errors or omissions in this *Accepted Manuscript* or any consequences arising from the use of any information it contains.



Journal Name

COMMUNICATION

## Facet-Dependent Catalytic Activity of ZIF-8 Nanocubes and Rhombic Dodecahedra Based on Tracing Substrate Diffusion in Pores by SERS: A Case Study for Surface Catalysis of MOFs

Received 00th January 20xx,  
Accepted 00th January 20xx

DOI: 10.1039/x0xx00000x

Liyong Chen,\* Binhua Duan, Qiong Luo, Zhizhi Gu, Jing Liu and Chunying Duan\*

www.rsc.org/

**We employed ZIF-8 rhombic dodecahedra and nanocubes as catalysts for insights into surface catalysis of MOFs based on facet-dependent catalytic activity for Knoevenagel condensation. The location of catalytic reactions was identified by using spiky Au@ZIF-8 single-core structures as surface-enhanced Raman scattering active substrate for aldehyde detection.**

The use of metal-organic frameworks (MOFs) as heterogeneous catalysts for a wide range of chemical reactions has attracted intriguing attention due to their tunable compositions and structures for easy introduction of catalytic sites into pores.<sup>1</sup> Exploiting their internal structures has been a conventional way to upgrade the catalytic performance of MOFs, but the effect of their external surface structures has been seldom discussed. Unsaturated coordination metal ions on external surfaces can serve as Lewis acidic catalytic sites with higher activity compared to saturated coordination metal ions of internal pores.<sup>2</sup> Therefore, well-understanding external surface catalysis provides the possibility to design MOF catalysts with extremely high catalytic activity for some specific reactions. On this basis, the well-defined MOF polyhedral shapes enclosed by different facets could be engineered for study on external surface catalysis. To achieve the purpose, MOFs should possess high chemical and thermal stability, and high symmetry crystal structures. Zeolitic imidazolate framework-8 (ZIF-8) with cubic sodalite-related structures to meet these needs can be employed as a candidate for elaborating facet-dependent catalytic activity.<sup>3</sup> In this research, we chose ZIF-8 in shapes of rhombic dodecahedron (named as RD) with {110} facets and nanocube (named as NC) with {100} facets with different densities of Zn<sup>2+</sup> ions as Lewis acid catalysts for Knoevenagel condensation. To the best of our knowledge, in many cases, identifying the location of catalytic sites was dependent on the size between

substrates and MOFs' pores. However, albeit some guest molecules were larger than the framework aperture in size, they could diffuse into the internal pores.<sup>4</sup> It was desirable to develop an effective strategy for probing the location of substrates while studying MOFs' surface catalysis. Surface-enhanced Raman scattering (SERS) has emerged as a powerful optical analytical tool for trace detection of molecules near the surface of plasmonic metal nanoparticles (NPs).<sup>5</sup> Herein, we design a SERS-active structure, single-core spiky Au@MOF composites, for exploration of substrate molecules diffusion behavior in MOFs' pores.

ZIF-8 rhombic dodecahedra (RDs) were prepared by mixing Zn(NO<sub>3</sub>)<sub>2</sub> and 2-methylimidazole (Hmim) in methanol and heating at 50 °C without perturbation for 2 h.<sup>6</sup> Transmission electron microscope (TEM) images (Fig. 1a and b) clearly reveal that the uniform ZIF-8 NPs are rhombic dodecahedral in shape with a narrow size distribution of about 135 nm (Fig. S1, ESI†). The polyhedral shapes are closely associated with facets in single crystal structure, and a complete RD is enclosed by twelve {110} planes. On the other hand, utilization of structure directing agents (SDAs) is a conventional method to control growth of NPs' crystal planes.<sup>7</sup> High-yield ZIF-8 NCs enclosed by six {100} facets with narrow size distribution were obtained by using hydrothermal synthesis while cetyltrimethylammonium bromide (CTAB) as a SDA was introduced into aqueous solution of Zn(NO<sub>3</sub>)<sub>2</sub> and Hmim.<sup>8</sup> The preferred attachment of CTAB molecules on {100} facets and thus resisting the growth of the facets cause ZIF-8 NCs formed. TEM images (Fig. 1d and e) reveal that the uniform ZIF-8 NCs of about 115 nm in size are synthesized (Fig. S1, ESI†). The crystal structures of both ZIF-8 nanocrystals are attributed to cubic sodalite-related structure crystallines that are determined by X-ray diffraction (XRD), and no impurity is observed from both XRD patterns (Fig. S2, ESI†). To elucidate the density of Zn<sup>2+</sup> ions of both facets, corresponding crystal structures observed from <110> and <100> direction are shown in Fig. 1c and f, respectively.

State Key Laboratory of Fine Chemicals, Dalian University of Technology, Dalian, 116024, PR China. E-mail: lyichen@dlut.edu.cn; cyduan@dlut.edu.cn

Electronic Supplementary Information (ESI) available: TEM images, Raman spectra, XPS spectra, XRD patterns, TG analysis, schematic illustrating of density and population of Zn<sup>2+</sup>, and experimental section. See DOI: 10.1039/x0xx00000x

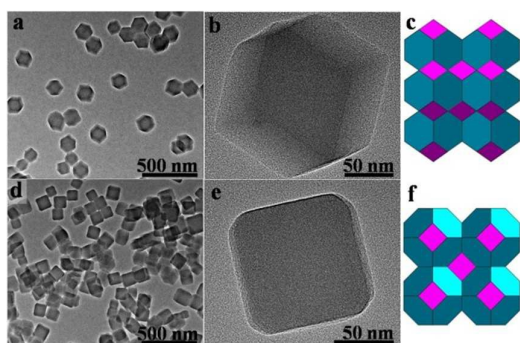


Figure 1. TEM images of well-defined ZIF-8 polyhedral nanocrystals: (a) and (b) rhombic dodecahedra, and (d) and (e) nanocubes with different magnification, respectively; topological structure of ZIF-8 observed along its crystallography (c)  $\langle 110 \rangle$  and (f)  $\langle 100 \rangle$  direction, respectively.

The terminated surface plane of ZIF-8 is the layer of  $\text{Zn}^{2+}$  ions that are bound into the bulk crystal structure by three mim (deprotonated Hmim) linkers.<sup>9</sup> The density of unsaturated  $\text{Zn}^{2+}$  ions at the apexes of polyhedra on  $\{110\}$  facets is 2.8 calculated from the unit cell; the density of  $\text{Zn}^{2+}$  ions increases to 4 for the  $\{100\}$  facets (Fig. S3, ESI<sup>†</sup>).<sup>8</sup> The population of Lewis acidic sites is equal to the product of surface density of  $\text{Zn}^{2+}$  ions and total external surface area. Owing to porous structures, the external surface area cannot be determined by  $\text{N}_2$  isothermal sorption technique separately (Fig. S4, ESI<sup>†</sup>), but a statistical calculation is possible to estimate it. Each ZIF-8 NC (115 nm) possesses almost the same external surface area as each ZIF-8 RD (135 nm), and for the identical amount of ZIF-8 nanocrystals, the number of ZIF-8 NCs is about 1.14 times than that of ZIF-8 RDs. Thus the total external surface area of ZIF-8 NCs is slightly larger than that of RDs (about 1.14 times). In contrast, the total population of external surface unsaturated coordination  $\text{Zn}^{2+}$  ions in NCs is about 1.68 times as much as that in RDs based on the density of  $\text{Zn}^{2+}$  ions in both facets and external surface area (Fig. S5, ESI<sup>†</sup>).<sup>17</sup>

Note that to eliminate the potential effect on catalytic activity as a result of molecule attachment on the external surface, ZIF-8 nanocrystals have to be pre-treated before use. In this regard, ZIF-8 NCs were firstly dispersed into a large amount of methanol to stir for 2 d at room temperature to remove CTAB. The surface component is determined by X-ray photoelectron spectroscopy (XPS). ZIF-8 NCs and RDs exhibited similar XPS survey spectra. In high-resolution N1s XPS spectrum of ZIF-8 NCs, the peak at around 401.5 eV of N1s binding energy corresponding to quaternary ammonium salt was not able to be found. The peak at 68.5 eV of Br3d binding energy was also absent in ZIF-8 NCs (Fig. S6, ESI<sup>†</sup>). These results suggest that CTAB molecules are dissociated from ZIF-8 NC surfaces after stirring in methanol. Moreover, in order to further exclude other molecules adsorbed on  $\text{Zn}^{2+}$  ions, both ZIF-8 samples were annealed at 300 °C in nitrogen atmosphere. It is worth noting that ZIF-8 is still stable at 300 °C according to thermal analysis (Fig. S7, ESI<sup>†</sup>). The original polyhedral ZIF-8 nanocrystals are maintained after heat treatment, characterized by TEM (Fig. 2a and b) and XRD (Fig. S8, ESI<sup>†</sup>).

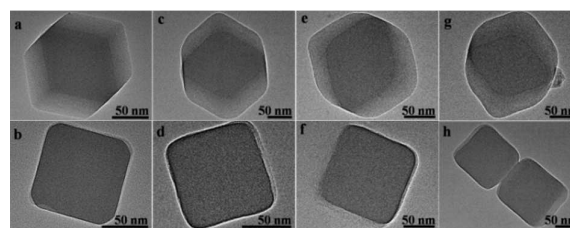


Figure 2. TEM images of ZIF-8 rhombic dodecahedrons and nanocubes by (a, b) annealing at 300 °C and catalytic reaction for (c, d) 10 min, (e, f) 30 min and (g, h) 1 h.


To study facet-dependent catalytic activity of ZIF-8 for Knoevenagel condensation, a suspension, containing ZIF-8, and substrates, malononitrile and benzaldehyde (molar ratio: 1:2), in toluene/ethanol (v/v = 3.5:0.5) solvent, was subjected to shaking for different durations at room temperature. The reaction is terminated by introducing acetone, and the conversion efficiency is analyzed by gas chromatography (GC) for measuring the amount of aldehyde converted. It was observed that quantitative conversion of benzaldehyde was about 73% after 10 min while using ZIF-8 NCs as catalyst. The conversion on ZIF-8 RDs decreased to 68% with identical reaction conditions. After 30 min, the conversion of benzaldehyde on ZIF-8 NCs was 94% slightly higher than that on RDs (93%). Benzaldehyde was consumed completely upon both catalysts till to 1 h (Table 1).

When ZIF-8 nanocrystals are used to study the facet-dependent catalytic activity, the stability of catalysts should be taken into consideration due to leaching of the species, including  $\text{Zn}^{2+}$  ions and mim ligands, from solid ZIF-8 to liquid phase. These leaching species providing potential active sites are responsible for the condensation according to their Lewis acid and Lewis base properties.<sup>10</sup> Thus, the leaching behavior adds ambiguity for estimation of catalytic activity of both ZIF-8 samples. To determine the stability of ZIF-8 in catalytic process, we performed time-dependent morphological and structural characterization of two types of catalysts for Knoevenagel condensation. Damaged surfaces of ZIF-8 nanocrystals were not found from the magnified TEM images (Fig. 2c-h) after catalytic reactions, following clear outlines of polyhedral shapes. The edges of polyhedra, however, are turned into less sharp with the progress of reaction for 1 h. XRD patterns of these samples are identical to as-synthesized ZIF-8 samples (Fig. S8, ESI<sup>†</sup>). In the catalytic process, stable planes and crystalline structures are key factors in exploration of surface-dependent catalytic performance. The leaching  $\text{Zn}^{2+}$  ions were further detected by inductively coupled plasmon atomic emission spectroscopy (ICP-AES). Zn element was not found while catalytic reaction for 10 min and 30 min, but trace Zn element ( $\sim 0.06$  wt% with respect to ZIF-8 RDs;  $\sim 0.05$  % with respect to ZIF-8 NCs) was measured in solution after 1 h of catalytic reaction.

To further affirm whether catalytic species were leached, ZIF-8 was removed from catalytic system after reacting for 10 min. The rest of mixture was shaken an additional 1 h. The conversion of benzaldehyde is not obviously changed, suggesting that leaching of ZIF-8 hardly occurs and the

contribution of catalytic reaction from mim and  $Zn^{2+}$  leached in solution can be ignored. Accordingly, ZIF-8 was removed from reaction mixture after 1 h, the following leaching experiment was also carried out by introducing extra benzaldehyde (100  $\mu$ L) due to the substrate depletion in catalytic process. A very small amount of the newly-added substrate was converted while extending to another 1 hour, indicating that a few catalytic species were leached from ZIF-8. Hence, to investigate the facet-dependent catalytic activity of ZIF-8, the reaction needs to be limited over a short period of time. As such, if reaction time reducing to 2 and 5 min, the conversion of benzaldehyde was decreased to 54% and 67% in presence of ZIF-8 NCs and 44% and 56% in presence of ZIF-8 RDs (Table 1).

Table 1. Knoevenagel condensation of malononitrile and aromatic aldehyde



Entry	Catalyst <sup>a</sup>	t [min]	Conversion <sup>b</sup> [%]		
			28/17	54/44	84/80
1		2	28/17	54/44	84/80
2		5	35/28	67/56	93/92
3	ZIF-8 NCs/RDs	10	45/44	73/68	>99/99
4		30	74/71	94/93	100/100
5		60	100/100	100/100	~

<sup>a</sup>Reaction conditions: 4.4 mol% ZIF-8 nanocrystals in ethanol/toluene solvents (3.5 mL) related to aldehyde (0.95 mmol), shaking for different durations at room temperature. <sup>b</sup>Conversion was determined by GC using n-dodecane as internal standard.

Knoevenagel condensation is very sensitive to aldehyde substrates. To understand the effect of substrates on the reaction, aldehyde substrates were extended to *p*-substituted benzaldehyde, including electron-withdrawing group ( $-NO_2$ ) and electron-donating group ( $-CH_3$ ). In contrast to other aromatic aldehydes, 4-nitrobenzaldehyde generally exhibited enhanced reactivity, and was almost completely consumed after reaction for only 10 min whatever ZIF-8 NCs or RDs as catalysts (Table 1). Correspondingly, both ZIF-8 nanocrystals exhibited lower catalytic activity for Knoevenagel condensation of malononitrile and 4-methylbenzaldehyde as compared to other aromatic aldehyde under the identical conditions. More interestingly, the time-dependent conversions of aldehyde, including 4-methylbenzaldehyde, benzaldehyde and 4-nitrobenzaldehyde, in ZIF-8 NC suspension are much higher than that in ZIF-8 RD suspension. They are about 1.65, 1.23, and 1.05 times larger than ZIF-8 RDs at the initial reaction of 2 min for the respective aldehydes (Table 1). On basis of these results, ZIF-8 NCs possess higher catalytic performance for different aldehydes.

The identical amount of ZIF-8 NCs and RDs should possess the same number of catalytic sites theoretically, and exhibit the similar catalytic performances for the same substrates. Therefore, we speculate that internal pores of ZIF-8 could not involve in catalyzing Knoevenagel condensation due to the size

of aldehyde being larger than that of pore apertures (0.34 nm) of ZIF-8 (Fig. S9, ESI<sup>†</sup>). To confirm the speculation, we engineer a single-core spiky Au@ZIF-8 heterostructures by a seed-mediated growth process to investigate the diffusion behavior of aromatic aldehydes, monitored by SERS spectra (Fig. 3a and b).<sup>6,11</sup> Owing to strain energy inducing by lattice mismatch between core and shell, only multifaceted crystallites of ZIF-8 shells can be obtained. Spiky Au NPs were allowed to generate many hotspots at sharp corners to localize electric field and 4-nitrobenzaldehyde was chosen as SERS tags due to weak interaction of nitro group with Au NPs.<sup>12</sup> If 4-nitrobenzaldehyde diffused into ZIF-8 pores and approached Au NPs within several nanometers, the Raman intensity was enhanced by localized electric field although spiky Au NPs were modified by a small amount of polyvinylpyrrolidone molecules (Fig. 3c). Au@ZIF-8 nanocomposites were incubated in 4-nitrobenzaldehyde ethanolic solution with different periods of time. The characteristic Raman peaks of 4-nitrobenzaldehyde cannot be found after incubating for 1 h. When the incubation time increasing to 12 h,  $NO_2$  stretching band ( $1344\text{ cm}^{-1}$ ) and phenyl ring breathing band ( $1596\text{ cm}^{-1}$ ), as well as C=O stretching band ( $1704\text{ cm}^{-1}$ ), are appeared. The intensity gradually enhanced while prolonging incubation time to 18 and 24 h.<sup>13</sup> If using the excitation frequency of 785 nm laser instead of 633 nm laser according to a previous report,<sup>14</sup> the Raman signals of 4-nitrobenzaldehyde were not allowed to be observed. In contrast to spiky Au@ZIF-8, pure ZIF-8 nanocrystals were not capable of visualizing the diffusion behavior of aldehyde molecules based on the change of Raman signals (Fig 3d). In light of the SERS results, 4-nitrobenzaldehyde is retarded to enter the cavity by apertures of ZIF-8.

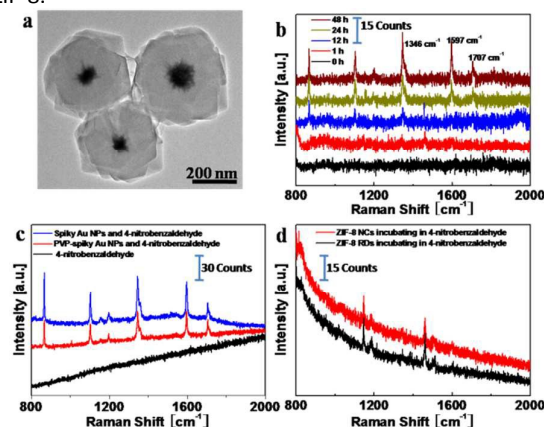


Figure 3. TEM image of (a) spiky Au@ZIF-8 heterostructures and Raman spectra of 4-nitrobenzaldehyde with (b) spiky Au@ZIF-8 heterostructures, (c) spike Au nanoparticles and (d) ZIF-8 nanocrystals. Excitation of 633 nm laser for all Raman tests.

Therefore, Knoevenagel condensation of aldehyde with malononitrile catalyzed by activated sites in cavity is restricted. Unsaturated coordination  $Zn^{2+}$  ions located at the external surfaces of ZIF-8 are considered as catalytic sites after heat treatment. The  $Zn^{2+}$  ions coordinating with malononitrile is an important step towards Knoevenagel reaction, and is

confirmed by cyano group stretching band in Raman spectroscopy (Fig. S10, ESI †) The intermediates are immobilized on the active sites in favor of the deprotonation of  $-\text{CH}_2-$  for subsequent condensation reaction.<sup>15</sup> The adjacent  $\text{Zn}^{2+}$  ions separated by 6 Å can interact with two N atoms of malononitrile. In toluene/acetonitrile, weak catalytic performance of ZIF-8 NCs for Knoevenagel reaction (conversion of benzaldehyde 47% after 10 min) could be attributed to competition of acetonitrile with malononitrile to adsorb on the Lewis acid sites.<sup>16</sup> Therefore, the different catalytic performance between ZIF-8 NCs and RDs could be attributed to the difference of population of  $\text{Zn}^{2+}$  ions on their external surfaces. Albeit both ZIF-8 nanocrystals with similar external surface areas, ZIF-8 NCs possess higher density of unsaturated coordination  $\text{Zn}^{2+}$  ions, leading to enhanced catalytic activity for Knoevenagel condensation.

The proposal catalytic mechanism should be attributed to  $\text{Zn}^{2+}$  ion-induced deprotonation behavior of active  $-\text{CH}_2-$ .<sup>17</sup> First, two negatively charged N atoms of malononitrile are allowed to interact with two corresponding  $\text{Zn}^{2+}$  ions, leading to the formation of much more positively charged  $\alpha\text{-H}$  of  $-\text{CH}_2-$  group with stronger acidity.<sup>15</sup> Second, the activated  $\alpha\text{-H}$  is lost from malononitrile, resulting in the formation of a hydron and a carbanion stabilized by  $\text{Zn}^{2+}$  ions. Third, the active carbonyl carbon atom attacks to the carbanion to form a carbon-carbon bond and the hydron polarizes the carbonyl group of aldehyde to produce a hydroxyl group. Finally, the dehydration occurs on the intermediate by combination of hydroxyl group with another  $\alpha\text{-H}$  of malononitrile, accounting for the formation of a carbon-carbon double bond, and then adducts are obtained by desorption of N atoms from  $\text{Zn}^{2+}$  ions and catalytic sites of ZIF-8 are recovered (Figure 4).

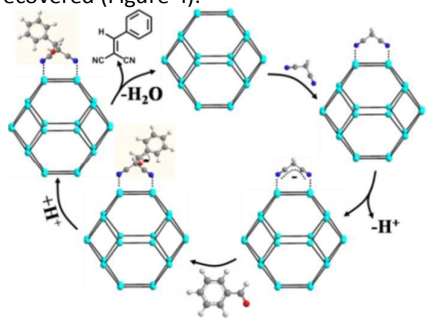


Figure 4. The proposal mechanism of Knoevenagel condensation catalyzed by ZIF-8.

In summary, the facet-dependent catalytic properties of MOFs have been systematically investigated through design and synthesis of well-defined ZIF-8 NCs and RDs. In combination with SERS spectra of bulky aromatic aldehydes, the external surface  $\text{Zn}^{2+}$  ions that coordinated with three N atoms of mim ligands were used as acidic sites for Knoevenagel condensation. Although identical amount of ZIF-8 RDs and NCs possessed similar external surface areas in our study, ZIF-8 NCs exhibit an enhanced catalytic performance in both samples due to much higher density of unsaturated coordination  $\text{Zn}^{2+}$  ion on {100} facets. The novel catalytic model gives insights into catalysis of external surfaces in porous materials, which is greatly

desirable for construction of MOF catalysts with fascinating performance for some specific organic reactions.

## Acknowledgements

We gratefully acknowledge financial support from the Foundation for Innovative Research Groups of the National Natural Science Foundation of China (21421005), the Specialized Research Fund for the Doctoral Program of Higher Education of China (20130041120025), the Fundamental Research Funds for the Central Universities (DUT15LK04), and the Foundation of the Ministry of Education of China for Returned Scholars.

## Notes and references

- 1 A. Corma, H. Garcia and F. X. L. Llabres i Xamena, *Chem. Rev.*, 2010, **110**, 4606.
- 2 (a) L. Chen, Q. Chen, M. Wu, F. Jiang and M. Hong, *Acc. Chem. Res.*, 2015, **48**, 201; (b) C. Chizallet, S. Lazare, D. Bazer-Bachi, F. Bonnier, V. Lecocq, E. Soyer, A.-A. Quoineaud and N. Bats, *J. Am. Chem. Soc.*, 2010, **132**, 12365; (c) C. V. McGuire and R. S. Forgan, *Chem. Commun.*, 2015, **51**, 5199.
- 3 K. S. Park, Z. Ni, A. P. Cote, J. Y. Choi, R. Huang, F. J. Uribe-Romo, H. K. Chae, M. O'Keeffe and O. M. Yaghi, *Proc. Natl. Acad. Sci. U.S.A.*, 2006, **103**, 10186.
- 4 J. V. Morabito, L.-Y. Chou, Z. Li, C. M. Manna, C. A. Petroff, R. J. Kyada, J. M. Palomba, J. A. Byers and C.-K. Tsung, *J. Am. Chem. Soc.*, 2014, **136**, 12540.
- 5 S. Schluecker, *Angew. Chem. Int. Ed.*, 2014, **53**, 4756.
- 6 L. Chen, Y. Peng, H. Wang, Z. Gua and C. Duana, *Chem. Commun.*, 2014, **50**, 8651.
- 7 A. Gole and C. J. Murphy, *Langmuir*, 2008, **24**, 266.
- 8 Z. Li and H. C. Zeng, *Chem. Mater.*, 2013, **25**, 1761.
- 9 P. Y. Moh, P. Cubillas, M. W. Anderson and M. P. Attfield, *J. Am. Chem. Soc.*, 2011, **133**, 13304.
- 10 (a) A. Pande, K. Ganesan, A. K. Jain, P. K. Gupta and R. C. Malhotra, *Org. Process Res. Dev.*, 2005, **9**, 133; (b) P. S. Rao and R. V. Venkataratnam, *Tetrahedron Lett.*, 1991, **32**, 5821.
- 11 A. M. Fales, H. Yuan and T. Vo-Dinh, *Langmuir*, 2011, **27**, 12186.
- 12 A. Corma, P. Concepcion and P. Serna, *Angew. Chem. Int. Ed.*, 2007, **46**, 7266.
- 13 (a) W. Xie, C. Herrmann, K. Koempe, M. Haase and S. Schluecker, *J. Am. Chem. Soc.*, 2011, **133**, 19302; (b) A. M. Amado and P. J. A. Ribeiro-Claro, *J. Raman Spectrosc.*, 2000, **31**, 971.
- 14 L. Rodriguez-Lorenzo, R. A. Alvarez-Puebla, F. Javier Garcia de Abajo and L. M. Liz-Marzan, *J. Phys. Chem. C*, 2010, **114**, 7336.
- 15 M. Polozij, M. Rubes, J. Cejka and P. Nachtigall, *Chemcatchem*, 2014, **6**, 2821.
- 16 U. P. N. Tran, K. K. A. Le and N. T. S. Phan, *ACS Catal.*, 2011, **1**, 120.
- 17 (a) J. D. Bass, S. L. Anderson and A. Katz, *Angew. Chem. Int. Ed.*, 2003, **42**, 5219; (b) S. L. Hruby and B. H. Shanks, *J. Catal.*, 2009, **263**, 181.